Characterization and reversal of synaptic defects in the amygdala in a mouse model of fragile X syndrome

Aparna Suvrathan[a], Charles A. Hoeffer[b], Helen Wong[b], Eric Klann[b], and Sumantra Chattarji[a,1]

[a]National Centre for Biological Sciences, Bangalore 560065, India; and [b]Center for Neural Science, New York University, New York, NY 10003

Edited* by William T. Greenough, University of Illinois, Urbana, IL, and approved May 5, 2010 (received for review February 22, 2010)

Fragile X syndrome (FXS), a common inherited form of mental impairment and autism, is caused by transcriptional silencing of the fragile X mental retardation 1 *(FMR1)* gene. Earlier studies have identified a role for aberrant synaptic plasticity mediated by the metabotropic glutamate receptors (mGluRs) in FXS. However, many of these observations are derived primarily from studies in the hippocampus. The strong emotional symptoms of FXS, on the other hand, are likely to involve the amygdala. Unfortunately, little is known about how exactly FXS affects synaptic function in the amygdala. Here, using whole-cell recordings in brain slices from adult *Fmr1* knockout mice, we find mGluR-dependent long-term potentiation to be impaired at thalamic inputs to principal neurons in the lateral amygdala. Consistent with this long-term potentiation deficit, surface expression of the AMPA receptor subunit, GluR1, is reduced in the lateral amygdala of knockout mice. In addition to these postsynaptic deficits, lower presynaptic release was manifested by a decrease in the frequency of spontaneous miniature excitatory postsynaptic currents (mEPSCs), increased paired-pulse ratio, and slower use-dependent block of NMDA receptor currents. Strikingly, pharmacological inactivation of mGluR5 with 2-methyl-6-phenylethynyl-pyridine (MPEP) fails to rescue either the deficit in long-term potentiation or surface GluR1. However, the same acute MPEP treatment reverses the decrease in mEPSC frequency, a finding of potential therapeutic relevance. Therefore, our results suggest that synaptic defects in the amygdala of knockout mice are still amenable to pharmacological interventions against mGluR5, albeit in a manner not envisioned in the original hippocampal framework.

autism | long-term potentiation | synaptic plasticity | metabotropic glutamate receptor

Fragile X syndrome (FXS), the most common inherited form of mental retardation, is caused by the lack of FMRP, the protein product of the fragile X mental retardation 1 (*Fmr1*) gene (1–3). A particularly useful framework for studying the cellular and molecular underpinnings of FXS has come from the "mGluR theory," which proposes that various symptoms of the disorder are triggered by a loss of translational regulation exerted by FMRP on the group I metabotropic receptor (mGluR) signaling pathway. One of the major findings leading to the mGluR theory is that in the hippocampus the group 1 mGluR receptor, mGluR5, is involved in long-term depression (LTD), a form of synaptic plasticity that is enhanced in the *Fmr1* knockout (*Fmr1* KO) mouse (4, 5). The underlying basis for this enhanced hippocampal mGluR-LTD is abnormally high internalization of the AMPA receptor (AMPAR) subunit, GluR1, caused by the absence of the end-point inhibition normally provided by FMRP (2, 6). Interestingly, defective AMPAR-mediated plasticity has also emerged as a common phenotype in other brain areas in the *Fmr1* KO mouse, including the cortex and cerebellum (7–11). However, such deficits are not limited to LTD, but are also frequently manifested as an impairment of long-term potentiation (LTP) (7, 12–15). Such LTP, expressed through AMPAR-dependent currents, does not always involve mGluR5 in its induction (8, 12, 16).

A majority of the observations contributing to the mGluR theory are derived from studies focusing primarily on the hippocampus and cortex (4, 7, 13, 14). The strong emotional symptoms of FXS, on the other hand, are likely to involve the amygdala (2, 13, 17). Unfortunately, little is known about the impact of FXS on synaptic function in the amygdala. This lack of knowledge, in turn, limits our ability to interpret earlier behavioral studies on anxiety and fear in the *Fmr1* KO mouse, which have yielded mixed results that are not consistent with the enhanced emotional symptoms observed in the human disease (17–20). Furthermore, whether or not synaptic abnormalities in the amygdala are consistent with the mGluR theory also remains unexplored. This issue is particularly relevant in light of previous reports on the contrasting nature of mGluR-dependent synaptic plasticity in the hippocampus versus amygdala. In area CA1 of the hippocampus, mGluR5 is involved in LTD, which is enhanced in *Fmr1* KO mice. In the lateral amygdala (LA), by contrast, mGluR5 mediates LTP. If the mGluR theory holds true in the amygdala, then it would predict the excessive mGluR signaling to cause enhanced mGluR-LTP in the LA of *Fmr1* KO mice. However, the same form of LTP (21) underlies classical fear conditioning, which, according to some reports, is impaired in *Fmr1* KO mice (17). This raises the possibility that mGluR-LTP too is impaired in the LA of mutant mice, which is opposite to the enhanced mGluR-LTP predicted by the mGluR theory. On the other hand, more recent studies in the hippocampus have shown that enhanced mGluR signaling leads to a reduction in surface levels of AMPARs; if a similar mechanism is in play in the amygdala, it could work against the stabilization of LTP in the LA (7, 14). A better understanding of the state of synaptic transmission and plasticity in the amygdala of mutant mice is needed to examine these divergent predictions. Therefore, the aim of the present study is to address some of these key issues within the broader context of the mGluR theory, using a combination of electrophysiological and biochemical analyses in the lateral amygdala of adult *Fmr1* KO mice.

Results

LTP Is Impaired at Thalamic Afferents to the LA in *Fmr1* KO Mice. We first focused on a key prediction of the mGluR theory by investigating if mGluR-LTP is indeed enhanced in the LA of *Fmr1* KO mice. To this end, we used whole-cell recordings to monitor excitatory postsynaptic potentials (EPSPs) evoked by stimulation of thalamic inputs to LA pyramidal cells in brain slices prepared from adult mice. In LA slices from WT mice, two trains of 100 pulses at 30 Hz led to robust LTP (average EPSP slope at minutes 40–45; 1.42 ± 0.13, numbers as mean ± SEM, normalized to baseline, $n = 6$). In WT slices, similar to reports in rats (21), this LTP was completely blocked by the specific mGluR5-antagonist 2-methyl-6-phenylethynyl-pyridine (MPEP, 40 μM)

Author contributions: A.S., C.A.H., E.K., and S.C. designed research; A.S., C.A.H., and H.W. performed research; A.S. and C.A.H. analyzed data; and A.S., E.K., and S.C. wrote the paper.

The authors declare no conflict of interest.

*This Direct Submission article had a prearranged editor.

[1]To whom correspondence should be addressed. E-mail: shona@ncbs.res.in.

This article contains supporting information online at www.pnas.org/lookup/suppl/doi:10.1073/pnas.1002262107/-/DCSupplemental.

(Fig. S1*E*). Strikingly, the same induction protocol failed to elicit any significant LTP in slices prepared from mutant littermates (1.03 ± 0.09, $n = 6$), (Fig. 1 *A* and *B*). Thus, in contrast to greater mGluR-LTD seen in the hippocampus, mGluR-LTP is impaired in the LA of *Fmr1* KO mice.

Next, we examined if this LTP deficit could be caused by abnormal action potential firing in LA neurons, because mGluRs are known to underlie pathological firing patterns in the hippocampus of *Fmr1* KO mice (22). We detected no difference in EPSP-Spike (E-S) coupling, an index of the probability of firing an action potential for a given synaptic strength (Fig. S1 *A* and *B*). Furthermore, action potentials, evoked by somatic injection of depolarizing currents, did not differ between KO and WT cells (Fig. S1 *C* and *D*), suggesting that deficits in postsynaptic excitability are unlikely to interfere with the induction of LTP in the LA of *Fmr1* KO mice.

Surface GluR1 Is Reduced in the LA of *Fmr1* KO Mice. Does this impairment, instead of enhancement, of mGluR-dependent synaptic plasticity in the amygdala of *Fmr1* KO mice contradict the mGluR theory? Recent studies have shown that the debilitating impact of excess signaling through mGluR5, caused by a loss of the translational repressor FMRP, is manifested in the hippocampus as enhanced internalization of the AMPAR subunit, GluR1 (6, 9, 23); it is this abnormally high AMPAR internalization that leads to greater hippocampal mGluR-LTD in *Fmr1* KO mice. If a similar mechanism is in play in the amygdala, it would undermine the stabilization of LTP by impairing insertion of AMPARs into synapses. We examined this possibility by quantifying levels of biotin-labeled surface GluR1 in basolateral amygdalar slices from *Fmr1* KO and WT mice by comparing both biotinylated GluR1 and total GluR1 protein. We found a reduction in GluR1 surface expression in *Fmr1* KO mice (KO: $73.2 \pm 7.9\%$, $n = 11$; WT: $100 \pm 7.2\%$, $n = 9$), (Fig. 1 *C*–*E*). Importantly, the difference was specific to surface-labeled GluR1 because total GluR1 protein was not different between WT and KO mice (KO: $99.9 \pm 7.5\%$; WT: $100 \pm 2.4\%$). Thus, although the direction of activity-induced change in synaptic strength and its aberration in *Fmr1* KO mice are opposite in the LA compared with the hippocampus, the reduction in AMPAR surface expression in the amygdala is in agreement with earlier findings in the cortex and hippocampus in *Fmr1* KO mice (6, 7).

The mGluR-Specific Inverse Agonist MPEP Fails to Rescue the LTP Deficit in the LA. The mGluR theory also proposes that inhibiting mGluR-activity should reverse defects observed in the *Fmr1* KO mice. We tested this by repeating the same 30-Hz LTP experiments in KO slices that were preincubated for 1 h in 40 μM MPEP, an mGluR5-specific inverse agonist, at concentrations that have earlier been used to reverse phenotypes in the *Fmr1* KO mice (6). Surprisingly, treatment with MPEP failed to reverse the impaired LTP observed in LA neurons from KO mice (normalized EPSP slope at minutes 30–35; WT: 1.41 ± 0.11; KO: 0.98 ± 0.11, $n = 6$; KO+MPEP: 1.11 ± 0.06, $n = 5$) (Fig. 2*A*). To further analyze this apparent contradiction of the mGluR theory in the amygdala, we took note of earlier findings from other brain areas of *Fmr1* KO mice exhibiting deficient forms of LTP that are not necessarily dependent on mGluR5 (7, 10, 11, 15, 16). Because restoration of AMPARs to the surface could also be mediated by other non-mGluR plasticity mechanisms, we wanted to ensure that contributions from such mechanisms are not constrained by our use of the 30 Hz mGluR-LTP induction protocol alone. Hence, to rule out the possibility that the 30-Hz stimuli may not be robust enough to recruit and stabilize AMPARs to the surface (16), we increased the frequency of tetanic stimulation to 100 Hz (24). In WT cells, this resulted in greater magnitude of LTP (1.74 ± 0.19, $n = 5$)

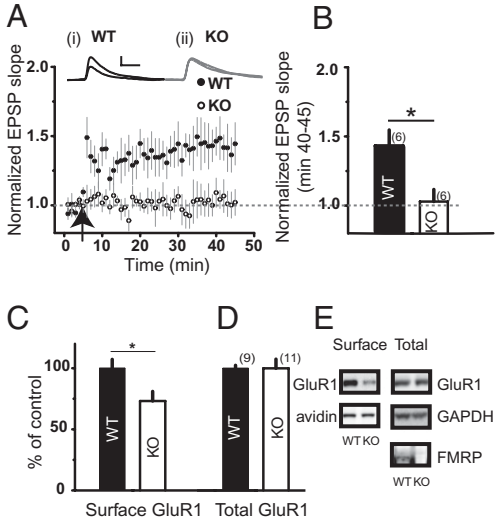

Fig. 1. mGluR5-dependent LTP is absent and surface GluR1 is reduced in the amygdala of *Fmr1* KO mice. (*A*) High-frequency stimulation at 30 Hz (arrow) induces LTP in LA slices from WT mice but not *Fmr1* KO siblings. (*Insets*) Average of 10 traces before tetanus and up to 45th minute: (*i*) WT (*ii*) KO. (Scale bars: 5 mV, 50 ms.) (*B*) Mean values of LTP from minutes 40 to 45, normalized to the 5-min pretetanus baseline. **P* = 0.033 (number of cells). (*C*) Surface expression of GluR1, determined by pull-down of biotin-labeled receptor, is reduced in KO mice. **P* = 0.024, (number of mice). (*D*) Total GluR1 is not different. (*E*) Representative Western blots are shown. Surface GluR1 is normalized to avidin, and total GluR1 to GAPDH. FMRP is absent in tissue from KO mice.

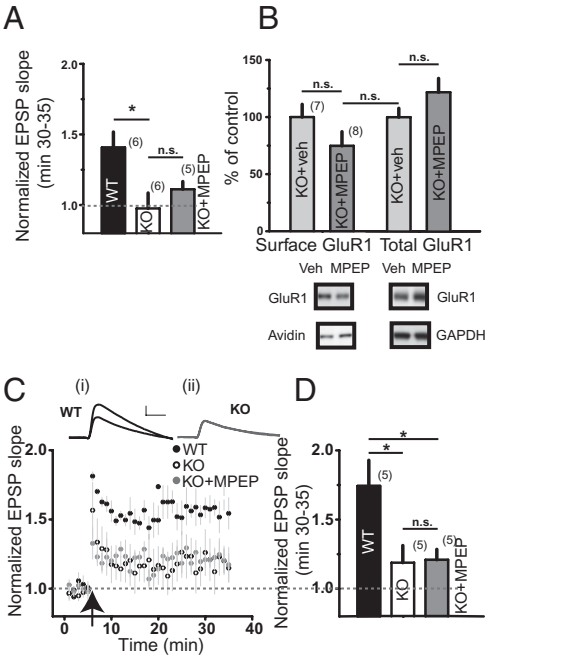

Fig. 2. Neither the LTP deficit nor reduction in surface GluR1 is rescued by MPEP. (*A*) MPEP (40 μM) treatment fails to rescue deficit in 30 Hz-LTP in KO cells. Mean values of LTP from minutes 30 to 35, normalized to the 5-min baseline. **P* = 0.019. (Number of cells) (*B*) MPEP preincubation does not change surface or total GluR1 levels in KO mice. (Number of mice) (*C*) LTP induced by 100-Hz tetanic stimuli (arrow) in WT slices is greater than KO slices; this deficit is not reversed by MPEP treatment. (*Insets*) Average of 10 traces before tetanus and up to 35th minute: (*i*) WT (*ii*) KO. (Scale bars: 5 mV, 50 ms.) (*D*) Mean values of LTP from minutes 30 to 35, normalized to 5-min pretetanus. One-way ANOVA **P* = 0.022, post hoc Tukey's HSD *P* values: WT-KO = 0.034, WT-KO+MPEP = 0.042 (number of cells).

(Fig. 2*C*) at thalamic inputs compared with the earlier 30-Hz protocol. Even this robust form of LTP was still significantly suppressed in *Fmr1* KO neurons and was not reversed by MPEP preincubation (normalized EPSP slope at minutes 30–35; KO: 1.19 ± 0.12, $n = 5$; KO+MPEP: 1.21 ± 0.08, $n = 5$), (Fig. 2 *C* and *D*).

Reduction in Surface GluR1 Is Also Not Reversed by MPEP in the LA of *Fmr1* KO Mice. We next probed the underlying basis of this failure to rescue impaired LTP in the LA of *Fmr1* KO mice by quantifying surface GluR1 after preincubation with MPEP. Again, as with the LTP experiments, amygdalar slices from *Fmr1* KO mice were preincubated for a period of 1 h in either 40 μM MPEP or vehicle. Strikingly, MPEP failed to restore AMPARs to the surface (surface GluR1; KO+vehicle: 100 ± 1.2%, $n = 7$; KO+MPEP: 74.78 ± 12.4%, $n = 7$), or to change total GluR1 (KO+vehicle: 100 ± 7.8%; KO+MPEP: 121.9 ± 12.1) (Fig. 2*B*). These results explain why postsynaptic expression of LTP in *Fmr1* KO mice is disrupted irrespective of the strength of the induction protocol. We also tested if this lack of effect was because of variations in mGluR5 plasticity or expression in the amygdala. In contrast to the hippocampus (23, 25), bath application of the group 1 mGluR-agonist dihydroxyphenylglycine (DHPG) (50 μM) in LA slices did not affect frequency and amplitude of spontaneous miniature AMPAR-mediated EPSCs, (mEPSCs) (Fig. S2 *A* and *B*). Levels of mGluR5 receptors were not different between KO and WT slices (Fig. S2*C*). Thus, mGluR5 receptors are available at comparable levels for MPEP to act; the effects of the selective agonist, however, appear to differ.

LA Neurons from KO Mice Exhibit Both Post- and Presynaptic Deficits in Excitatory Synaptic Transmission. Despite identifying a clear impairment in synaptic plasticity, the results presented thus far provide no insights into the overall status of basal synaptic transmission in the amygdala in the *Fmr1* KO brain. Moreover, we have no corroboration of the electrophysiological consequences of the postsynaptic deficit in the levels of surface AMPARs. Therefore, we compared the frequency and amplitude of mEPSCs in LA slices from KO and WT mice (Fig. 3 *A*–*C*). Miniature AMPAR-mediated EPSCs were recorded in the presence of tetrodotoxin (TTX) and picrotoxin, and were completely blocked by 6-cyano-7-nitroquinoxaline-2,3-dione (CNQX), showing that they were AMPAR-dependent synaptic currents (Fig. S1*F*). *Fmr1* KO neurons exhibited a significant reduction in mEPSC frequency (WT: 0.68 ± 0.13 Hz, $n = 22$; KO: 0.2 ± 0.03 Hz, $n = 20$) (Fig. 3*B*), as well as amplitude (WT: 23.4 ± 0.77 pA; KO: 20.8 ± 0.4 pA) (Fig. 3*C*). Although the decrease in mEPSC amplitude together with the reduction in surface AMPARs points to postsynaptic deficits, the decrease in mEPSC frequency in KO cells may be indicative of presynaptic effects. To ensure that this deficit was specifically present at the thalamic inputs where we earlier found LTP to be impaired, thalamic afferents were stimulated and extracellular Ca^{2+} was replaced with Sr^{2+}, resulting in an evoked synchronous EPSC along with a barrage of desynchronized miniature EPSCs (SrEPSCs) (Fig. 3*D*, *Inset*). SrEPSC amplitude was significantly reduced in KO mouse slices (WT: 23.96 ± 0.8 pA, $n = 6$; KO: 21.65 ± 0.5 pA, $n = 8$). Therefore, the deficit in surface AMPARs was indeed present at the thalamic synapses in the LA.

Having obtained biochemical and electrophysiological measures of postsynaptic deficits that are in agreement, we turned our attention to the reduction in mEPSC frequency in LA neurons in the *Fmr1* KO mice, which is suggestive of changes in presynaptic release probability. To test this possibility we measured paired-pulse ratios across a range of interstimulus intervals, at the thalamic inputs to the LA. We found paired-pulse facilitation ratios of evoked EPSCs are greater in KO mice compared with the absence of paired-pulse facilitation in WT mice, indicating a reduction in release probability in *Fmr1* KO neurons (WT: $n = 6$; KO: $n = 6$) (Fig. 3*E*). The reduction in mEPSC frequency, along

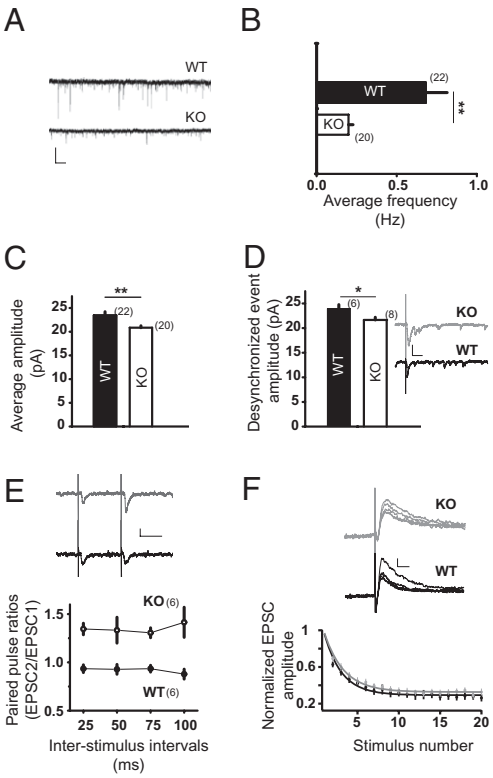

Fig. 3. LA cells exhibit reduced frequency and amplitude of mEPSCs, enhanced paired-pulse facilitation, and slower MK-801-induced decays in *Fmr1* KO mice. (*A*) Sample mEPSC traces. (Scale bar: 20 pA, 1s.) (*B*) Summary of change in frequency. $^{**}P = 0.002$. (*C*) Summary of change in amplitude. $^{**}P = 0.005$. (*D*) Strontium-desynchronized events evoked by stimulation of thalamic inputs to the LA show reduced amplitude in KO mice. $^{*}P = 0.029$. (*Inset*) Sample traces. (Scale bars: 50 pA, 0.02 s.) (*E*) Enhanced paired-pulse facilitation in KO (○) compared with WT cell (●). $^{**}P = 0.006$, (repeated measures ANOVA). (*Inset*) Sample of averaged EPSC traces at 100-ms interstimulus interval. (Scale bars: 20 pA, 0.05 s.) (Number of cells). (*F*) Release probability is lower at thalamic inputs to LA in KO mice. Normalized amplitude of the NMDA-EPSC is plotted after bath application of 40 μM MK-801. Progressive block of the NMDA-EPSC by MK-801 is slower at KO synapses (gray) compared with WT synapses (black) in the LA. (*Inset*) Sample traces of first five EPSCs in MK-801. (Scale bars: 50 pA, 0.02 s.)

with greater paired-pulse facilitation ratios, warrants a more rigorous analysis of the decrease in probability of release (P_r), especially because no such presynaptic effect has been reported in the hippocampus. Hence, thalamic inputs to the LA were repeatedly stimulated in the presence of the NMDAR open-channel blocker (5S,10R)-(+)-5-methyl-10,11-dihydro-5H-dibenzo[a, d]cyclohepten-5,10-imine maleate (MK-801). This led to a progressive decay of NMDAR-EPSCs (Fig. 3*F*), the time constant of which is inversely related to P_r. The decay kinetics were fit by a double exponential, and the fast time-constant of decay (τ_f) compared across groups (26, 27). MK-801 blockade led to a slower τ_f, implying a lower P_r in KO cells [WT: 0.78 ± 0.32, $n = 7$; KO: 1.86 ± 0.24, $n = 7$ (stimuli); $P < 0.05$] (Fig. 3*F*).

MPEP Reverses Reduction in mEPSC Frequency but Not mEPSC Amplitude in the LA. Taken together, the electrophysiological and biochemical data presented so far point to both pre- and postsynaptic deficits in *Fmr1* KO neurons. Although MPEP did not reverse deficits in postsynaptic surface AMPARs in the LA, could it nonetheless rescue the presynaptic deficit in release probability? We investigated this by repeating the mEPSC recordings in KO slices that were preincubated for 1 h in 40 μM of MPEP. Surprisingly, MPEP was indeed able to return mEPSC

frequency in *Fmr1* KO neurons to levels not significantly different from WT neurons (WT: 0.68 ± 0.13 Hz, $n = 22$; KO: 0.2 ± 0.03 Hz, $n = 20$; KO+MPEP: 0.48 ± 0.02 Hz, $n = 13$) (Fig. 4 *A* and *C*); but mEPSC amplitude was not altered by MPEP (WT: 23.4 ± 0.77 pA; KO: 20.8 ± 0.4 pA; KO+MPEP: 22 ± 0.72 pA) (Fig. 4 *B* and *D*). Although the lack of reversal of amplitude in *Fmr1* KO neurons supports our earlier observation on the lack of recovery of AMPARs to the surface with the biotinylation assay (Fig. 2*B*), the reversal of the mEPSC frequency deficit in *Fmr1* KO neurons implicates changes in presynaptic release that are amenable to rescue by MPEP treatment.

Discussion

Although the results presented herein are consistent with certain aspects of the mGluR theory, they also underscore the need to modify the existing framework to better explain synaptic dysfunction in the amygdala in a mouse model of FXS, where mGluR-signaling differs from the hippocampus (2). The mGluRs in the LA are involved in LTP, not LTD (Fig. 5) (21). Furthermore, hippocampal mGluR-LTD is larger in KO mice (4), but we report the opposite effect in the amygdala. Another prediction of the mGluR theory also does not hold up in the amygdala: neither the LTP deficit, nor the reduced surface expression of AMPARs, was rescued by MPEP treatment (Fig. 5). Yet, despite its failure to reverse the postsynaptic defects, MPEP treatment for the same duration was able to reverse mEPSC frequency in the LA. In contrast, in the hippocampus, MPEP treatment rescues the postsynaptic deficit in surface AMPARs (6), but no presynaptic changes in transmitter release have been reported in *Fmr1* KO mice (Fig. 5).

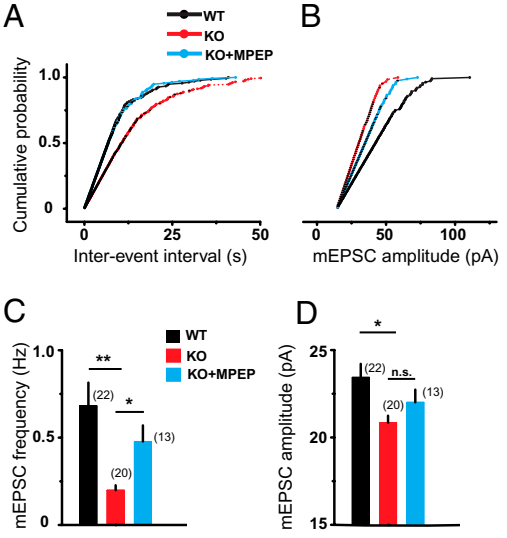

Fig. 4. LA Deficits in presynaptic release are reversed by acute MPEP treatment. (*A*) Preincubation of LA slices from *Fmr1* KO mice in 40 μM MPEP and reversal of decreased mEPSC frequency: cumulative probability of mEPSC interevent intervals (IEI). The *x* axis truncated at IEI of 50,000 ms. IEIs averaged within 100-ms bins, then across cells, and normalized. K-S test, significance levels $P < 0.0001$ between WT-KO and MPEP-KO, $P = 0.999$ between WT-MPEP. (*B*) Cumulative probability of mEPSC amplitudes. Bin size 0.5 pA. K-S test, $P < 0.0001$ between WT-KO, $P = 0.016$ between WT-MPEP, and $P = 0.163$ between KO and MPEP. (*C*) Summary of across-cell comparisons: MPEP preincubation reverses reduction in mEPSC frequency in KO cells. One-way ANOVA with Welch's statistic $P = 0.001$. Post hoc pairwise Games-Howell test: *Fmr1* KO-WT $^{**}P = 0.005$; MPEP-treated KO-KO $^{*}P = 0.029$; MPEP-treated KO-WT: $P = 0.439$. (*D*) LA cells in KO slices have lower mEPSC amplitude. One-way ANOVA $P = 0.018$ (Post hoc pairwise Games-Howell test *, $P = 0.015$). Reduction in mEPSC amplitude is not rescued by MPEP preincubation (number of cells).

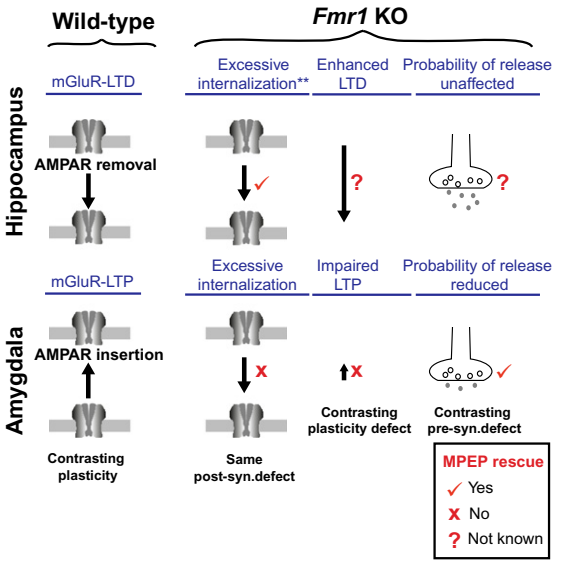

Fig. 5. Summary of results in the LA of *Fmr1* KO mice and how they differ from those reported earlier in the hippocampus. MPEP treatment reverses some phenotypes (ticks), but fails to rescue others (cross); absence of data, ?. **Contradictory findings (6, 28, 32).

Despite these contrasts, we find a common endpoint underlying synaptic defects in the amygdala and other brain regions. Our analysis uncovers the same deficit in surface AMPARs in the LA (Fig. 5). The significant reduction in AMPAR surface expression, in turn, works against the establishment of robust LTP in the LA, irrespective of the strength of the induction protocol. This finding is also in agreement with studies reporting suppression of LTP caused by impaired surface delivery of AMPARs in the cortex of *Fmr1* KO mice (8). In the hippocampus, however, AMPAR-internalization triggered by mGluR-LTD adds to the reduced surface AMPARs in *Fmr1* KO cells to give rise to greater LTD (Fig. 5).

Our results also point to additional differences between the amygdala and hippocampus within the broader context of the mGluR theory and FXS. For example, the basal level of surface AMPARs is lower in the LA of KO mice, but in the hippocampus earlier results appear to be mixed (6, 28). However, both of these studies have relied on acute molecular manipulations in cultured hippocampal neurons that are likely to differ from brain tissue in which disease-induced changes have stabilized over the course of development into adulthood. Thus, the synaptic defects identified herein are likely to reflect changes linked directly to the loss of FMRP, as well as homeostatic changes compensating for such synaptic dysfunction. Future studies will be needed to examine if the pre- and postsynaptic deficits reported here evolve in a particular sequence or in parallel.

Although earlier studies have focused on postsynaptic defects, the reduction of mEPSC frequency, and its reversal with MPEP, highlight the need to further investigate changes in presynaptic release probability in the LA of *Fmr1* KO mice. This issue is noteworthy for several reasons. Past studies on cellular phenotypes of the *Fmr1* KO mouse have focused largely on postsynaptic aberrations. In contrast to our results, no presynaptic effects have been reported in the hippocampus or cortex of KO mice. Moreover, in the LA, mGluR5 is localized to the postsynaptic side (21). Therefore, an important question arises: how does postsynaptic mGluR5 provide a basis for presynaptic deficits and their reversal in KO slices? Not enough is known to answer this question in the amygdala, but earlier studies in the hippocampus suggest possible mechanisms. For example, activation of postsynaptic mGluR5 and p38 MAP kinase leads to

a reduction in presynaptic release in the hippocampus (29–31). Of particular relevance to the present study is the existence of a developmental switch for pre- versus postsynaptic changes in hippocampal mGluR-LTD (27). Specifically, although mGluR-LTD at neonatal synapses results in a significant reduction in presynaptic release probability without any postsynaptic effects, at mature synapses it causes a decrease in AMPAR surface expression without any detectable change in presynaptic function (27). In the hippocampus, this framework has been used to show that mGluR-LTD in *Fmr1* KO mice is the mature, postsynaptic form (32). By contrast, in the adult LA we observe reduced AMPAR surface expression to coexist with lower mEPSC frequency, which is indicative of a decrease in release probability. Thus, what is seen as a "neonatal" deficit in presynaptic function in the hippocampus may not undergo the same developmental switch in the mature amygdala, and thereby continue to function like a developmentally arrested immature synapse. This in turn is consistent with the view that a hallmark of FXS is deficient synaptic maturation (33, 34).

Even with the divergent manifestations of abnormal synaptic transmission and plasticity in the amygdala versus hippocampus, our results suggest that synaptic defects in the amygdala of *Fmr1* KO mice are still amenable to pharmacological interventions against mGluR5, albeit in a manner not envisioned in the original framework of the mGluR theory. This theory is noteworthy in light of the previously reported reversal of behavioral deficits by MPEP (35). Hence, future studies based on this framework will have to take into account both pre- and postsynaptic effects, as well as their brain region-specific variations. Despite these challenges, of particular significance is our finding that even a relatively brief treatment with an mGluR5-antagonist is capable of correcting a key aspect of deficient transmission on the presynaptic side that has received relatively little attention in earlier studies. A genetic approach has previously been used to prevent FXS symptoms in mice through chronic reduction in mGluR expression from birth (36), but our results raise the exciting possibility that this reversal can be achieved pharmacologically even after the disease has had months to leave its mark in the adult brain.

Materials and Methods

Animals. Adult *Fmr1* KO mice and WT siblings were provided by the Tonegawa and Bear laboratories at the Picower Centre for Learning and Memory, Massachusetts Institute of Technology (MIT, Cambridge, MA). Animals were genotyped in MIT, as previously described (37). They were housed with siblings with a 14-h/10-h day/night cycle with ad libitum access to food and water.

Slice Preparation. Male *Fmr1* KO mice or age-matched WT siblings (3.5–6 mo old) were used following National Centre for Biological Sciences/New York University institutional Animal Ethics Committee-approved procedures. Animals were anesthetized with Halothane, cervically dislocated, and decapitated. The brain was dissected under ice-cold artificial cerebrospinal fluid (aCSF: 124 mM NaCl, 2.7 mM KCl, 2 mM $CaCl_2$, 1.3 mM $MgCl_2$, 26 mM $NaHCO_3$, 0.4 mM NaH_2PO_4, 18 mM glucose and 4 mM ascorbate; pH 7.3, 290 mOsm) and whole-brain coronal slices (350 μm) obtained using a Vibratome 1000 Plus. Slices were transferred to a submerged chamber containing aCSF equilibrated with 95% O_2 and 5% CO_2. The slices were incubated at room temperature for at least 1 h before being transferred to a superfused recording chamber.

In Vitro Slice Electrophysiology. Whole-cell recordings were performed at 28 to 30 °C for all mEPSC, PPF, SrEPSC, and E-S coupling experiments. Slices were held at 24 °C for LTP and MK-801 recordings. Neurons were visually identified with infrared videomicroscopy using an upright microscope equipped with a 60× objective (Olympus BX50WI, water immersion lens, 0.9 N.A.). Patch electrodes (3-6 MΩ) were pulled from borosilicate glass tubing and filled with a solution containing 120 mM potassium gluconate, 20 mM KCl, 10 mM Hepes buffer, 10 mM phosphocreatine, 4 mM Mg-ATP, and 0.3 mM Na-GTP (pH 7.25; 295 mOsm). For voltage-clamp experiments, potassium was replaced by equimolar cesium. In current-clamp recordings, membrane potential was kept manually at −74 mV. Data were recorded with an HEKA EPC9 (HEKA Elektronik) amplifier, filtered at 2.9 kHz and digitized at 10 kHz. Monosynaptic EPSPs or EPSCs were elicited by stimulation of thalamic afferent fibers with a bipolar twisted platinum/iridium wire (2 × 25 μm, FHC, Bowdoin). Series resistance was monitored throughout the experiment by applying hyperpolarizing current or voltage pulses, was less than 25 MOhms and did not change by more than 10% for mEPSC and desynchronized EPSC recordings and 25% for LTP and MK-801 recordings.

Long-Term Potentiation. High-frequency stimulation consisted of two trains of 100 pulses at 30 Hz, 20 s apart. Experiments were performed in 100 μM picrotoxin, and cortical inputs were cut off. Stimulation was at 0.05 Hz, and each minute was averaged for Figs. 1*A* and 2*C*. LTP was quantified for statistical comparisons by averaging and normalizing EPSP slopes during minutes 40 to 45 and minutes 30 to 35 to the 5-min baseline. For 100 Hz LTP, coronal slices were intact, and tetanus was one train of 200 pulses at 100 Hz. Quantification of LTP was by comparison of minutes 30 to 35 normalized to the 5-min baseline. Slopes were quantified using Igor Pro (Wave Metrics Inc.), setting cursors within the 10 to 90 range of EPSP slope during the baseline. The same cursor settings were maintained for slope measurements over the entire post-LTP time course. For LTP reversal experiments, coronal slices were preincubated in aCSF containing 40 μM MPEP for 1 h, before incubating in the recording chamber without MPEP for at least 15 min.

mEPSCs. For mEPSC experiments, 5 continuous min were used for analysis, beginning at least 4 min after the whole-cell recording configuration had been established. Experiments were performed in 100 μM picrotoxin and 0.5 μM TTX and analyzed using MiniAnalysis (Synaptosoft Inc.). The mEPSCs were completely blocked by 10 μM CNQX (Fig. S1*F*).

Paired-Pulse Ratios. Paired-pulse ratios were determined as the ratio of amplitudes of the second EPSC to the first, for a range of interstimulus intervals.

Strontium-Desynchronized EPSCs. LA cells held were at −70 mV and thalamic afferents were stimulated in the presence of 100 μM picrotoxin and 0.5 μM TTX. 2 mM Ca^{2+} in the aCSF was replaced with 2 mM Sr^{2+} and the initial synchronous EPSC decreased in size in parallel with an appearance of SrEPSCs (38, 39). EPSC amplitude stabilized in ≈15 min, and stimulation frequency was 2 Hz for 10 traces, repeated every 20 s (25). Asynchronous events were measured offline during the 740-ms period after stimulus, using MiniAnalysis (Synaptosoft Inc.). Desynchronized events were subjected to visual confirmation and 100 events were randomly selected from each cell for amplitude analysis.

MK-801–Induced Decays of NMDAR Currents. NMDAR receptor mediated EPSCs evoked by thalamic stimulation were recorded at +40 mV in the presence of 10 μM CNQX and 100 μM picrotoxin. EPSCs were elicited every 15 s (26, 40). Next, 40 μM MK-801 was added to the perfusate and stimulation was paused for 10 min to allow it to equilibrate (26, 40). Stimulation was then resumed and the decay of NMDAR EPSC amplitudes measured. EPSC amplitudes were normalized to the first trace in MK-801. The first 30 traces of progressive blockade was fit to a double exponential in IgorPro. MK-801–induced NMDA-EPSC decays were the same for C57BL/6 mice and WT siblings, and these values were pooled before comparison with KO mice.

Statistical Analyses. All values are expressed as mean ± SEM. Statistical comparisons were done after using Levene's test and single sample K-S test for appropriate assumptions of variance and normality of distribution. Comparisons between two groups used the Student's *t* test. Multiple group comparisons for mEPSCs were done using one-way ANOVA, with the Welch statistic for unequal variances (41), followed by post hoc Tukey's or Games-Howell pairwise tests. Distributions were compared using the K-S test.

Reagents. Picrotoxin and CNQX were obtained from Sigma-Aldrich. MPEP hydrochloride was a gift from FRAXA Research Foundation, TTX was from Alomone Labs. MK-801 maleate and DHPG were obtained from Tocris Biosciences.

Biochemical Analysis of Surface and Total GluR1. ***Amygdalar slice preparation.*** Mice were killed and coronal slices (400 μm) were obtained using a Leica VT1200 microtome and cutting solution (in mM: 110 sucrose, 11.6 Na L-ascorbic acid, 60 NaCl, 2.5 KCl, 25 $NaHCO_3$, 1.25 NaH_2PO_4, 7 $MgCl_2$, 2.5 D-glucose, 0.5 $CaCl_2$). Slices containing amygdala were allowed to recover for 30 min in saturated 95% O_2:5% CO_2 solution of 50:50 cutting solution:aCSF (in mM: 125 NaCl, 2.5 KCl, 25 $NaHCO_3$, 1.25 NaH_2PO_4, 1 $MgCl_2$, 25 D-glucose, 2 $CaCl_2$) at 25 °C. Slices were then transferred to aCSF at 32 °C for 1 h incubation before labeling. For MPEP

treatment, following recovery slices were incubated with 40 μM MPEP or vehicle (aCSF) for 60 min before biotin surface labeling. Slice biotinylation, streptavidin pull-down, and Western blotting were done following standard procedures, using the antibodies listed below. Details of the procedures are described in *SI Materials and Methods*. Data represent mean + SEM.

Antibodies. Antibodies used were: goat anti biotin-HRP (Pierce) 1:500; mouse anti-MAP2 (Abcam) 1:2,000; goat anti-mouse-HRP (Promega) 1:5,000; mouse anti-avidin (Abcam) 1:5,000; rabbit anti-GAPDH (Novus) 1:10,000; mouse anti-FMRP (Chemicon) 1:1,000; rabbit monoclonal anti-mGluR5 (Novus) 1:1,000; goat anti-rabbit-HRP (Promega) 1:5,000.

ACKNOWLEDGMENTS. We thank Candice Carr, Bridget Dolan, Kathleen Oram, and others at the Tonegawa and Bear laboratories (Picower Institute for Learning and Memory, Massachusetts Institute of Technology, Cambridge, MA) for genotyping and providing us the mice. This work was supported by funds from the FRAXA Research Foundation, a Pfizer Asia R and D collaborative grant, and the National Centre for Biological Sciences, Bangalore.

1. Bassell GJ, Warren ST (2008) Fragile X syndrome: Loss of local mRNA regulation alters synaptic development and function. *Neuron* 60:201–214.
2. Bear MF, Huber KM, Warren ST (2004) The mGluR theory of fragile X mental retardation. *Trends Neurosci* 27:370–377.
3. Ronesi JA, Huber KM (2008) Metabotropic glutamate receptors and fragile X mental retardation protein: Partners in translational regulation at the synapse. *Sci Signal* 1:pe6.
4. Huber KM, Gallagher SM, Warren ST, Bear MF (2002) Altered synaptic plasticity in a mouse model of fragile X mental retardation. *Proc Natl Acad Sci USA* 99:7746–7750.
5. Hou L, et al. (2006) Dynamic translational and proteasomal regulation of fragile X mental retardation protein controls mGluR-dependent long-term depression. *Neuron* 51:441–454.
6. Nakamoto M, et al. (2007) Fragile X mental retardation protein deficiency leads to excessive mGluR5-dependent internalization of AMPA receptors. *Proc Natl Acad Sci USA* 104:15537–15542.
7. Li J, Pelletier MR, Perez Velazquez JL, Carlen PL (2002) Reduced cortical synaptic plasticity and GluR1 expression associated with fragile X mental retardation protein deficiency. *Mol Cell Neurosci* 19:138–151.
8. Hu H, et al. (2008) Ras signaling mechanisms underlying impaired GluR1-dependent plasticity associated with fragile X syndrome. *J Neurosci* 28:7847–7862.
9. Muddashetty RS, Kelić S, Gross C, Xu M, Bassell GJ (2007) Dysregulated metabotropic glutamate receptor-dependent translation of AMPA receptor and postsynaptic density-95 mRNAs at synapses in a mouse model of fragile X syndrome. *J Neurosci* 27: 5338–5348.
10. Koekkoek SK, et al. (2005) Deletion of FMR1 in Purkinje cells enhances parallel fiber LTD, enlarges spines, and attenuates cerebellar eyelid conditioning in fragile X syndrome. *Neuron* 47:339–352.
11. Larson J, Jessen RE, Kim D, Fine AK, du Hoffmann J (2005) Age-dependent and selective impairment of long-term potentiation in the anterior piriform cortex of mice lacking the fragile X mental retardation protein. *J Neurosci* 25:9460–9469.
12. Lauterborn JC, et al. (2007) Brain-derived neurotrophic factor rescues synaptic plasticity in a mouse model of fragile X syndrome. *J Neurosci* 27:10685–10694.
13. Zhao MG, et al. (2005) Deficits in trace fear memory and long-term potentiation in a mouse model for fragile X syndrome. *J Neurosci* 25:7385–7392.
14. Wilson BM, Cox CL (2007) Absence of metabotropic glutamate receptor-mediated plasticity in the neocortex of fragile X mice. *Proc Natl Acad Sci USA* 104:2454–2459.
15. Desai NS, Casimiro TM, Gruber SM, Vanderklish PW (2006) Early postnatal plasticity in neocortex of Fmr1 knockout mice. *J Neurophysiol* 96:1734–1745.
16. Meredith RM, Holmgren CD, Weidum M, Burnashev N, Mansvelder HD (2007) Increased threshold for spike-timing-dependent plasticity is caused by unreliable calcium signaling in mice lacking fragile X gene *FMR1*. *Neuron* 54:627–638.
17. Paradee W, et al. (1999) Fragile X mouse: Strain effects of knockout phenotype and evidence suggesting deficient amygdala function. *Neuroscience* 94:185–192.
18. Dobkin C, et al. (2000) Fmr1 knockout mouse has a distinctive strain-specific learning impairment. *Neuroscience* 100:423–429.
19. Schneider A, Hagerman RJ, Hessl D (2009) Fragile X syndrome — From genes to cognition. *Dev Disabil Res Rev* 15:333–342.
20. Harris SW, et al. (2008) Autism profiles of males with Fragile X syndrome. *Am J Ment Retard* 113:427–438.
21. Rodrigues SM, Bauer EP, Farb CR, Schafe GE, LeDoux JE (2002) The group I metabotropic glutamate receptor mGluR5 is required for fear memory formation and long-term potentiation in the lateral amygdala. *J Neurosci* 22:5219–5229.
22. Chuang SC, et al. (2005) Prolonged epileptiform discharges induced by altered group I metabotropic glutamate receptor-mediated synaptic responses in hippocampal slices of a fragile X mouse model. *J Neurosci* 25:8048–8055.
23. Snyder EM, et al. (2001) Internalization of ionotropic glutamate receptors in response to mGluR activation. *Nat Neurosci* 4:1079–1085.
24. Humeau Y, et al. (2007) A pathway-specific function for different AMPA receptor subunits in amygdala long-term potentiation and fear conditioning. *J Neurosci* 27: 10947–10956.
25. Oliet SH, Malenka RC, Nicoll RA (1997) Two distinct forms of long-term depression coexist in CA1 hippocampal pyramidal cells. *Neuron* 18:969–982.
26. Bender KJ, Allen CB, Bender VA, Feldman DE (2006) Synaptic basis for whisker deprivation-induced synaptic depression in rat somatosensory cortex. *J Neurosci* 26: 4155–4165.
27. Nosyreva ED, Huber KM (2005) Developmental switch in synaptic mechanisms of hippocampal metabotropic glutamate receptor-dependent long-term depression. *J Neurosci* 25:2992–3001.
28. Pfeiffer BE, Huber KM (2007) Fragile X mental retardation protein induces synapse loss through acute postsynaptic translational regulation. *J Neurosci* 27:3120–3130.
29. Bolshakov VY, Carboni L, Cobb MH, Siegelbaum SA, Belardetti F (2000) Dual MAP kinase pathways mediate opposing forms of long-term plasticity at CA3-CA1 synapses. *Nat Neurosci* 3:1107–1112.
30. Bolshakov VY, Siegelbaum SA (1994) Postsynaptic induction and presynaptic expression of hippocampal long-term depression. *Science* 264:1148–1152.
31. Fitzjohn SM, et al. (2001) A characterisation of long-term depression induced by metabotropic glutamate receptor activation in the rat hippocampus in vitro. *J Physiol* 537:421–430.
32. Nosyreva ED, Huber KM (2006) Metabotropic receptor-dependent long-term depression persists in the absence of protein synthesis in the mouse model of fragile X syndrome. *J Neurophysiol* 95:3291–3295.
33. Comery TA, et al. (1997) Abnormal dendritic spines in fragile X knockout mice: Maturation and pruning deficits. *Proc Natl Acad Sci USA* 94:5401–5404.
34. Weiler IJ, Greenough WT (1999) Synaptic synthesis of the fragile X protein: Possible involvement in synapse maturation and elimination. *Am J Med Genet* 83:248–252.
35. Yan QJ, Rammal M, Tranfaglia M, Bauchwitz RP (2005) Suppression of two major fragile X syndrome mouse model phenotypes by the mGluR5 antagonist MPEP. *Neuropharmacology* 49:1053–1066.
36. Dölen G, et al. (2007) Correction of fragile X syndrome in mice. *Neuron* 56:955–962.
37. Hayashi ML, et al. (2007) Inhibition of p21-activated kinase rescues symptoms of fragile X syndrome in mice. *Proc Natl Acad Sci USA* 104:11489–11494.
38. Goda Y, Stevens CF (1994) Two components of transmitter release at a central synapse. *Proc Natl Acad Sci USA* 91:12942–12946.
39. Hessler NA, Shirke AM, Malinow R (1993) The probability of transmitter release at a mammalian central synapse. *Nature* 366:569–572.
40. Fourcaudot E, et al. (2008) cAMP/PKA signaling and RIM1alpha mediate presynaptic LTP in the lateral amygdala. *Proc Natl Acad Sci USA* 105:15130–15135.
41. Oren I, Mann EO, Paulsen O, Hájos N (2006) Synaptic currents in anatomically identified CA3 neurons during hippocampal gamma oscillations in vitro. *J Neurosci* 26:9923–9934.